Theoret. Chim. Acta (Berl.) 37, 217—231 (1975)

Group-Theoretical Analysis of Carbonium Ion Rearrangements: The Barbaralyl Cation

Thomas D. Bouman

Department of Chemistry, Southern Illinois University, Edwardsville, IL 62025, USA

Carl Trindle*

Department of Chemistry, University of Virginia, Charlottesville, VA 22901, USA

Received June, 28, 1974/ September 23, 1974

The permutation group theory developed by Longuet-Higgins is applied to the degenerate rearrangement of the barbaralyl cation, $C_9H_9^+$. The analysis allows explicit solution of the kinetic equations for one possible rearrangement mechanism and the time evolution of the quantum-mechanical states of the system. Permutation symmetry constraints, imposed by the Pauli principle applied to interchange of spin-1/2 nuclei, lead to characteristic level splitting patterns, and to the exclusion of an intermediate proposed by Hoffmann and others [6, 7]. We discuss implications of these constraints for deciding among alternative mechanistic pathways.

Key words: Barbaralyl cation – Carbonium ion rearrangements – Group theory

1. Introduction

The familiar Pauli exclusion principle, requiring that the total wave function be antisymmetric upon interchange of electrons [1], applies as well to systems of indistinguishable fermion nuclei. The resulting symmetry constraint has observable consequences for the spectra of *ortho*- and *para*-H_2, NH_3 and similar systems [2]. Permutations of the nuclei in such molecules are effected by bodily rotation, and thus the permutation symmetry constraints are observed on a time scale comparable to the period of rotation.

We have previously explored several metallorganic and carbonium ion systems, in which permutation of identical fermion nuclei is brought about by rapid chemical processes rather than bodily rotations [3, 4]. We have deduced compatibility conditions between nuclear spin states and internal motional states that lead to distinct low- and high-temperature spin distributions. In the present work we apply group-theoretical and topological methods to a rapidly rearranging carbonium ion system, the so-called "barbaralyl" cation [5]. We will show that symmetry considerations make possible an explicit decoupling of the kinetic equations for one rearrangement mechanism, that vibrational-rotational levels are split into characteristic patterns by tunneling among equivalent potential-energy minima, and that one suggested intermediate is ruled out on grounds of symmetry [6, 7].

* Alfred P. Sloan Fellow, 1971–1973.

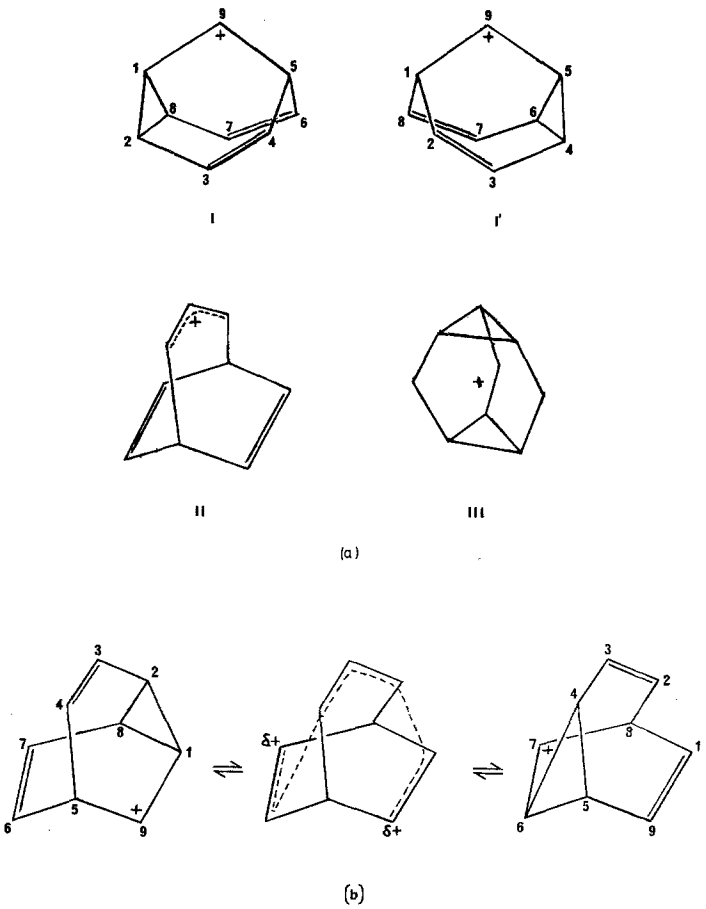

Fig. 1. (a) Structures and numbering conventions for barbaralyl isomers and intermediates referred to in text. (b) Concerted rearrangement in Mechanism 1

2. Rearrangement Mechanisms

The barbaralyl (tricyclo[3.3.1.$0^{2,8}$]nona-3,6-dien-9-yl) cation **I** (see Fig. 1) is known to undergo rapid degenerate rearrangement, even at temperatures of $-135°$ C [5]. A single line is observed in the nmr spectrum at this temperature, implying the barrier to rearrangement is $\leqq 6$ kcal/mole [8]. Four proposed mechanisms for this rearrangement have been listed by Leone *et al.* [5], two of which may be excluded on the basis of direct chemical and thermodynamic evidence. The remaining two mechanisms are[1]:

1) A synchronous, concerted migration of three bonds, reforming barbaralyl directly (see Fig. 1b).

2) Conversion of **I** to a $\mathscr{C}_{2v}$ intermediate bicyclo[3.2.2]nonatrienyl cation (**II**), followed by a 1,2 vinyl shift and/or rearrangement to a degenerate isomer of **I**.

[1] Leone *et al.* [5] number these 4 and 1, respectively.

The existence of **II** as the actual lowest-energy intermediate has been called into question recently on the basis of approximate MO calculations [7].

Either of these processes may be coupled with a rapid degenerate Cope rearrangement (**I**⇌**I**′).

Because the rearrangement, by whatever process, is degenerate, any of the isomers may be obtained formally from any other by a simple permutation of the nuclei that leaves the molecular skeleton unchanged. The set of permutations describing all isomers encountered in a particular sequence of rearrangements forms a group. We therefore apply a group theoretical analysis to the system, and look for symmetry-aided insights into the kinetic behavior of the system, as well as possible constraints on the fluxional motion.

3. Group Theory of the Barbaralyl Cation

Molecules whose potential energy surface contains many equivalent minima with low barriers to rearrangement can not be adequately described by the point group of any one isomer. The methods of Ruch and Hässelbarth [9], and Klemperer [10] based on double coset enumeration have provided an elegant and powerful means of discussion of possible mechanistic pathways in such systems. However, since our aim is not to enumerate possible mechanisms, but rather to assess possible permutational symmetry constraints involving the Pauli principle, we find that the "molecular symmetry group" (MSG) formalism defined by Longuet-Higgins [11, 12] allows a symmetry analysis of these systems more directly suited to the present discussion[2].

To facilitate discussion of barbaralyl, we name the various degenerate isomers as follows: Denote each skeletal position by a number, as in **I** (Fig. 1). A particular isomer is named by listing, in order, the (labeled) atoms occupying those positions. Thus the isomer **I** will be labeled [1 2 3 4 5 6 7 8 9], while, for example, the result **I**′ of the Cope rearrangement becomes [5 6 7 8 1 2 3 4 9] after the molecule is rotated back into coincidence with the reference isomer. In permutation notation, the process **I**⇌**I**′ is denoted (15)(26)(37)(48). It is the labeled atoms that are permuted over fixed skeletal positions.

A single, unrearranged isomer has two symmetry elements: the identity E, and a "reflection", denoted by $(28)(37)(46)^* = \sigma^*$, in the notation of Ref. [11]. Addition of the "feasible" operation corresponding to the Cope rearrangement of **I** gives $(15)(26)(37)(48) = R$.

Mechanism 1 has one other generator, $R' = (14)(25)(39)(68)$, corresponding to the concerted rearrangement. Together with the other three elements, it generates a group of 12 elements, isomorphic with $\mathscr{D}_{3h}$. Table 1 lists the elements and divides them into classes.

Mechanism 2 has one new generator: $V = (173)(28)(496)$, the result of a 1,2-vinyl shift. This new operation, together with the four original ones, may be

[2] The "differentiable permutational isomerization reactions" of Klemperer are directly analogous to the "feasible permutations" described by Longuet-Higgins, apart from those related to static symmetry. However, chemical experience must be used to reduce the number of either to a manageable level: a Klemperer-type analysis of barbaralyl yields a total of 90, 792 differentiable permutational isomerization reactions, assuming $\mathscr{C}_s$ static symmetry, including many chemically unfeasible pairwise permutations. In any case, the mechanisms we treat are differentiable by any of the criteria mentioned.

Table 1. Molecular symmetry group for barbaralyl cation, generated by Mechanism 1

Class	Element
E	E
$2P^2$	$P^2 = (128)(379)(465)$
	$P^4 = (182)(397)(456)$
$3R$	$R = (15)(26)(37)(48)$
	$R' = (14)(25)(39)(68)$
	$R'' = (16)(24)(58)(79)$
P^3*	$P^3* = (15)(24)(68)*$
$2P*$	$P* = (162584)(397)*$
	$P^5* = (148526)(379)*$
$3\sigma*$	$\sigma* = (28)(37)(46)*$
	$\sigma'* = (12)(39)(45)*$
	$\sigma''* = (18)(56)(79)*$

shown to generate the full permutation-inversion group of nine particles, $\mathscr{S}_9 \times (E, E^*)$, with $2 \times 9! = 725,760$ elements. The same group is obtained whether or not one includes the Cope rearrangement as a distinct process.

The "starred" operations in these groups are not simple permutations of nuclei, but are permutations coupled with inversion of all particle coordinates through an origin. These operations are important in the description of electronic states of the system, but they are of no consequence in the description of nuclear motions and spin states for non-chiral systems. Hence the relevant subgroups are one with 6 elements, isomorphic with $\mathscr{C}_{3v}$, and the symmetric group $\mathscr{S}_9$, with 362,880 elements.

4. Symmetry Analysis of Mechanism 1

Any given isomer may convert to another in one of three ways: by the two symmetry equivalent concerted processes R' and R'', or by the Cope rearrangement R. (This notation, of course, refers only to the reference isomer. The appropriate geometrically equivalent operation is implied for other isomers.) Starting with the reference isomer [1 2 3 4 5 6 7 8 9], it is easily shown that the following 6 isomers are the only ones generated by this mechanism. For later convenience we list them in the following order, and assign each one an index.

1. [1 2 3 4 5 6 7 8 9],
2. [4 5 9 1 2 8 7 6 3] generated from 1. by R',
3. [8 1 9 5 6 4 3 2 7] generated from 1. by P^4,
4. [5 6 7 8 1 2 3 4 9] generated from 1. by R,
5. [2 8 7 6 4 5 9 1 3] generated from 1. by P^2,
6. [6 4 3 2 8 1 9 5 7] generated from 1. by R''.

The graph for the rearrangement process is shown in Fig. 2. Each vertex corresponds to an isomer, while each edge is a single mechanistic step. A sequence of such steps allows interconversion of any two of the six structures. Thus the graph is not the complete graph of the MSG, in the usual graph-theoretical sense, but rather the graph of "feasible direct tunneling processes", as defined by Dalton [12].

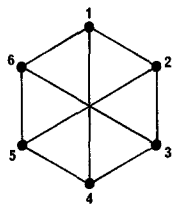

Fig. 2. Graph for Mechanism 1. Solid lines connect isomers interconnected by a single process. The lines across the diagonal correspond to the Cope rearrangement, while those on the perimeter refer to the concerted process

5. Solution of Kinetic Equations

The rate law expressing the time evolution of the concentration of the i^{th} isomer may be written

$$\frac{dC_i}{dt} = a(C_j + C_k) + bC_\ell - (2a+b)\,C_i\,, \tag{1}$$

where a and b are the rate constants for the concerted and Cope processes, respectively, and j, k, and ℓ index isomers adjacent to i on the graph. In matrix form [13], this becomes

$$\frac{d\underset{\sim}{C}}{dt} = [\underset{\sim}{A} + \underset{\sim}{B} - k\underset{\sim}{E}]\,\underset{\sim}{C}\,. \tag{2}$$

Here $\underset{\sim}{C}$ is a six-dimension column vector containing the concentrations of the six isomers, $\underset{\sim}{E}$ is the 6 x 6 unit matrix, $\underset{\sim}{A}$ and $\underset{\sim}{B}$ are 6 x 6 matrices, and $k = 2a + b$. $\underset{\sim}{A}$ and $\underset{\sim}{B}$ are found by noting, for each isomer, the three adjacent vertices on the graph, and placing the appropriate rate constants in the corresponding matrix elements. The result is given in Eq. (3).

$$\underset{\sim}{A} + \underset{\sim}{B} = \begin{pmatrix} . & a & . & b & . & a \\ a & . & a & . & b & . \\ . & a & . & a & . & b \\ b & . & a & . & a & . \\ . & b & . & a & . & a \\ a & . & b & . & a & . \end{pmatrix}. \tag{3}$$

The matrix sum $\underset{\sim}{A} + \underset{\sim}{B}$ is invariant under the group of the graph shown in Fig. 2, as verified by direct generation of all 6! possible permutations of the vertices, in matrix form, and testing for the solution of the equation $\underset{\sim}{P}^{-1}(\underset{\sim}{A} + \underset{\sim}{B})\,\underset{\sim}{P} = \underset{\sim}{A} + \underset{\sim}{B}$. This group, of order 12, is isomorphic with the MSG, but since no rearrangement process interconverts "starred' and "unstarred" isomers, it is appropriate to classify the eigenvectors with respect to the subgroup "$\mathscr{C}_{3v}$", shown in Table 2.

Using the methods of Brocas [13] we find that chemical "normal modes" which satisfy uncoupled first-order rate equations evolve with rate constants $\lambda_i = 0,\ -3a,\ -3a,\ -a-2b,\ -a-2b,\ -4a-2b$, all non-positive. The value

Table 2. Characters and species labels for "$\mathscr{C}_{3v}$"

"$\mathscr{C}_{3v}$"	E	$2P^2$	$3R$
A_1	1	1	1
A_2	1	1	−1
E	2	−1	0

$\lambda_i = 0$ corresponds to conservation of mass: the sum of all the concentrations does not change with time. The normal modes may be classed in "$\mathscr{C}_{3v}$" as A_1, E (twice), and A_2. All but the totally symmetric normal mode undergo first-order decay, each mode with its own characteristic relaxation time. The observed concentration changes may be inferred from the normal modes, as Brocas points out. All the changes depend on only two parameters, a and b, the rest being determined by symmetry.

6. Quantum-Mechanical Stationary States for the Rearrangement Process

Any symmetry constraints on the fluxional system must arise from the behavior of the quantum-mechanical stationary states of the system. In this section we show the formal relation between these states and the macroscopic "kinetic normal modes".

Let χ_μ represent the wave function of isomer μ. A rearrangement will then correspond to changing the description of the system to (say) χ_ν. Since the energy surface for the system has a number of equivalent minima separated by low energy barriers, none of the distinct functions χ describes any of the stationary states of the system. A particular isomer is described by a superposition of stationary states ϕ_k:

$$\chi_\mu = \sum_k \phi_k b_{k\mu} . \tag{4}$$

Conversely, a stationary state will be a linear combination of wave functions for the separate isomers:

$$\phi_k = \sum_\mu \chi_\mu b^\dagger_{\mu k} . \tag{5}$$

The matrix $\underset{\sim}{b}$ is assumed to be unitary.

The fluxional system, viewed as a whole, changes with time; its quantum-mechanical description will be

$$\psi(t) = \sum_\nu \chi_\nu a_\nu(t) = \sum_k \phi_k d_k(t) . \tag{6}$$

The coefficients $a_\nu(t)$ determine the relative amount of each isomer as a function of time; the macroscopic concentration, $C_\mu(t)$, of the μ^{th} isomer is given by

$$C_\mu(t) = \mathcal{N} a^*_\mu(t)\, a_\mu(t) , \tag{7}$$

where $\mathcal{N}$ is the total concentration of all species. (The assumption of a single accessible quantum-mechanical state for each isolated species is implicit here. At low temperatures, this will hold approximately. Extension of the argument to a sum over populated levels is straightforward.) Comparison of Eqs. (4) and (6) shows that $\underset{\sim}{a}$ and $\underset{\sim}{d}$ are related by $\underset{\sim}{a} = \underset{\sim}{b}^{+}\underset{\sim}{d}$.

The functions ϕ_k are assumed to satisfy the time-dependent Schrödinger equation

$$i\hbar \frac{\partial \phi_k}{\partial t} = \mathscr{H}_0 \phi_k = E_k \phi_k . \tag{8}$$

The time-dependence of the ϕ_k consists of a phase factor: $\phi_k = f_k \exp(-i\omega_k t)$, where $\omega_k = E_k/\hbar$, and f_k is independent of time.

The fluxional system description $\psi(t)$ also satisfies the time-dependent Schrödinger equation

$$i\hbar \frac{\partial \psi(t)}{\partial t} = [\mathscr{H}_0 + \mathscr{H}'(t)]\, \psi(t) , \tag{9}$$

where we have allowed the inclusion of a time-dependent perturbation to permit transitions between stationary states. $\mathscr{H}'(t)$ must have a Fourier component of frequency comparable with the energy separation between nearby stationary states. In these systems this separation will be small and $\mathscr{H}'$ will be weakly time-dependent. Substitution of Eq. (6) yields:

$$i\hbar \sum_k \dot{d}_k(t)\, \phi_k = \sum_k d_k(t)\, \mathscr{H}'(t)\, \phi_k . \tag{10}$$

Multiplication by ϕ_L^* and integration over space and time (from $t' = 0$ to t) gives:

$$d_L(t) - d_L(0) = (i\hbar)^{-1} \sum_k \int_0^t d_k(t') \langle \phi_L | \mathscr{H}'(t') | \phi_k \rangle \, dt' . \tag{11}$$

The initial condition is that the system consist of one particular isomer, i.e., that $\psi(0) = \chi_\varrho$, say, and therefore $d_k(0) = b_{k\varrho}$, all k. The time evolution in terms of particular isomers is obtained from Eqs. (4), (6), and (11):

$$a_\mu(t) - a_\mu(0) = (i\hbar)^{-1} \sum_{kL} \sum_{\sigma\nu\lambda} b^\dagger_{\mu L} b_{L\nu} b^\dagger_{\lambda k} b_{k\sigma} \int_0^t a_\sigma(t') \langle \chi_\nu | \mathscr{H}'(t') | \chi_\lambda \rangle \, dt' . \tag{12}$$

If the system is in state $\mu = \varrho$, the l.h.s. will be zero at first, but will become negative as contributions from other isomers σ grow in. For short times, the coefficients $a_\sigma(t')$ will be negligible except for isomers adjacent to μ on the graph. If $\mu = \varrho$ initially, the l.h.s. will grow with time, and the only appreciable term on the r.h.s. will be that with $\sigma = \varrho$. An iterative solution of Eq. (12) leads to a series expansion whose second and higher terms correspond to "transitions" between isomers two, three, etc., steps removed along the graph.

The interaction matrix elements $\langle \chi_\mu | \mathscr{H}'(t') | \chi_\nu \rangle$ may be plausibly assumed to vary only slowly with time, since the χ_ν are time-independent, and $\mathscr{H}'$ is dominated by low-frequency Fourier components. The time dependence of $a_\mu(t)$ is then approximated by a polynomial in t. The nature of this expansion may be deduced from the macroscopic kinetic equations: the concentrations $C_\mu(t)$ are

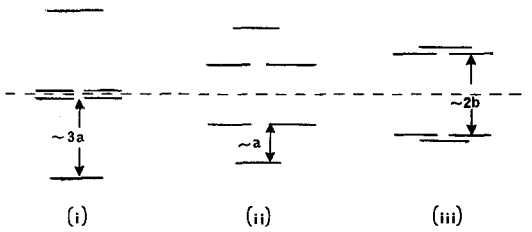

Fig. 3. Splitting patterns for eigenvalues from Mechanism 1. Case (i): $a \simeq b$; case (ii): $a \gg b$; case (iii): $a \ll b$. Eigenvalues are equally weighted about the center

expressible as a linear combination of exponential factors [13]; Eq. (7) implies the same behavior for the product $a_\mu^*(t)\, a_\mu(t)$.

The initial conditions imply that a number of excited stationary states must be populated in order to localize the system in a particular isomer. We assume that the decay from an excited state occurs exponentially, with some characteristic relaxation time; thus $d_k(t) = d_k(0) \exp(-t/\tau_k)$. From the relation between $\underset{\sim}{a}$ and $\underset{\sim}{d}$ we see that the r.h.s. of Eq. (7) is again expressible as a sum of exponential terms with different relaxation times, in consonance with the macroscopic behavior.

According to Eqs. (5) and (8), the variational solution for the ϕ_k leads to matrix elements $\langle \chi_\mu | \mathscr{H}_0 | \chi_\nu \rangle$. Using a Hückel-type approximation, we neglect all integrals connecting "non-adjacent" isomers. The remaining ones will be of two types: $\langle \chi_\mu | \mathscr{H}_0 | \chi_\nu \rangle = a$ for the concerted process, and b for the Cope rearrangement. The secular matrix then has a form identical with the matrix sum $\underset{\sim}{A} + \underset{\sim}{B}$ from the kinetic equations. We thus expect eigenvectors belonging to A_1, A_2, and E (twice). It is worth noting that, because of the form of the matrix in this case, the same invariance properties are obtained whether or not non-neighbor interactions are included. (In general, however, Hückel-type matrices may display higher symmetry than that implied by the quantum-mechanical Hamiltonian [14].)

Analogously to the potential energies of internal rotation or ammonia inversion, we are able to define local vibrational states in each of the several minima, split by the mixing of corresponding states of other minima. The splitting and thus the stationary states of the system can be described schematically by the eigenvalues and eigenvectors of the matrix $\langle \chi_\mu | \mathscr{H}_0 | \chi_\nu \rangle$. The eigenvalues are determined by (1) the magnitude of parameters a and b, and (2) the symmetry of the $\mathscr{H}_0$ matrix. Eigenvalues of the matrix for the "$\mathscr{C}_{3v}$" mechanism are sketched in Fig. 3, for cases where $a \gg b$, $a \sim b$, and $a \ll b$. The splitting is small relative to the vibrational spacing. Using the methods of Stejskal and Gutowsky [15], we estimate the splitting to be on the order of $10^{-3}\ \mathrm{cm}^{-1}$ for the ground state for motion in a local minimum and $10^{-1}\ \mathrm{cm}^{-1}$ for the first excited state in the local minimum. States within a band will be populated according to a Boltzmann distribution, implying that all components of a degenerate level are equally populated. Note that the kinetic asymptotic state, equal population of each isomer, does not necessarily imply that only the totally symmetric (A_1) microscopic state is occupied; equal population of each component of a degenerate level also produces uniform isomer population.

Table 3. Characters of the representations spanned by spin functions

"$\mathscr{C}_{3v}$"	E	$2P^2$	$3R$
(9, 0)	1	1	1
(8, 1)	9	0	1
(7, 2)	36	0	4
(6, 3)	84	3	4
(5, 4)	126	0	6

7. Nuclear Spin States and the Pauli Principle

The barbaralyl cation has the molecular formula $(CH)_9^+$, and thus consists of nine spin-$\frac{1}{2}$ (CH) fermion pseudoparticles. On a time scale long enough to allow many rearrangements but comparable to the time scale of an nmr experiment, say, the Pauli Principle governs the overall behavior of the wave function: that is, the wave function must be antisymmetric with respect to interchange of any pair of CH fragments. The total wave function for the system is written as a product of terms:

$$\psi_{\text{total}} = \psi_{\text{motion}} \psi_{\text{nuclear spin}} .$$

The "motional" part is composed of vibronic, rotational, and fluxional coordinates, which may be strongly coupled in a rapid rearrangement process. Examination of the character table shows that ψ_{total} must have A_1 symmetry to obey the Pauli principle, i.e., that $\Gamma_{\text{motion}} \times \Gamma_{\text{spin}} = A_1$.

The $2^9 = 512$ nuclear spin functions are classified by partitions (n_α, n_β), giving the respective number of α and β spins. For those sets with $n_\alpha > n_\beta$, we have 1 function in (9,0), 9 in (8,1), 36 in (7,2), 84 in (6,3), and 126 in (5,4). Spin functions that are simple products of α and β spins transform in a simple way under permutations. The characters of the representation of "$\mathscr{C}_{3v}$" generated by each partition are just the number of product functions left unchanged by the permutation. The characters are given in Table 3. When spin multiplicities are taken into account, the 512 spin functions are seen to span the following states: dectet A_1; octet $A_1 + A_2 + 3E$; sextet $6A_1 + 3A_2 + 9E$; quartet $9A_1 + 9A_2 + 15E$; and doublet $7A_1 + 5A_2 + 15E$.

The Pauli restriction produces the following statistical weights for the motional (rotational-fluxional) states: A_1:104, A_2:72, E:168. When a given isomer is formed, by solvolysis for example, the system is not in a stationary state, nor is the nuclear spin state well defined. After long times, when a stationary state is established, one would obtain the symmetry-dictated statistical weights. The selection rule for electric dipole transitions is $\Gamma_i \leftrightarrow \Gamma_i$ ($\vec{r}$ is totally symmetric in permutation groups). By assuming intensities proportional to the statistical weights of the levels, we calculate spectroscopic splitting patterns for the low-frequency vibrational transitions within a potential well. These are shown for various line widths in Fig. 4. If any resolution of the broad line is possible, the theoretical patterns allow one to decide on the relative magnitudes of the parameters a and b.

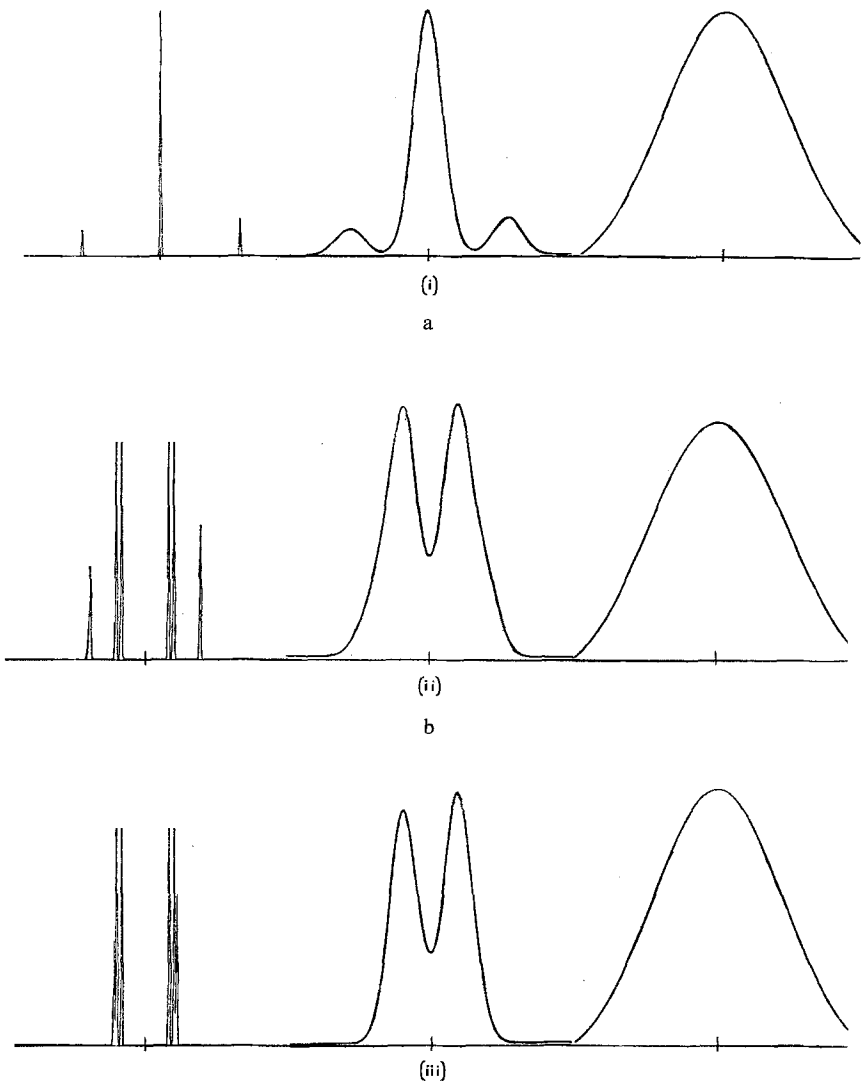

Fig. 4a–c. Calculated spectra for transitions between level patterns for the cases shown in Fig. 3. Upper-state values for a and b are 10 times the lower state values in each case. (i) $a = b$; (ii) $a = 10b$; (iii) $b = 10a$

Finally, we note that if the kinetic or quantum-mechanical parameters a and b are in fact the same, the matrix of Eq. (3) remains invariant under the full group of the graph. This group has 72 elements, and is isomorphic with the nmr symmetry group of ethane, whose character table is given by Woodman [16]. The "accidentally" fourfold degenerate tunneling levels [cf. Case (i) of Fig. 3] are seen to derive from the occurrence of a fourfold degenerate symmetry species of this group among the eigenvectors of the isomerization Hamiltonian matrix.

8. Analysis of a Proposed Intermediate

Hoffmann *et al.* [6], using Walsh orbital arguments, and Yoneda *et al.* [7] on the basis of CNDO calculations, have independently proposed a $\mathscr{D}_{3h}$ structure **III** as the mediator of both the Cope process and the concerted migration of Mechanism 1. A symmetry analysis of this proposal is possible, using the methods developed above.

Once the structure **III** is attained during traversal of the reaction coordinate, after a stationary state is formed, the symmetry of the potential surface implied by this structure assures that any of six collapse pathways are equally probable, each one leading to one of the six degenerate barbaralyl isomers discussed above. Then there exists a feasible direct tunneling process connecting each isomer with each of the others. The graph of the system of isomers is then the *complete* graph of six vertices, as shown in Fig. 5, and the interaction Hamiltonian matrix takes the form of Eq. (13).

$$\boldsymbol{H} = \begin{pmatrix} . & a & a & a & a & a \\ a & . & a & a & a & a \\ a & a & . & a & a & a \\ a & a & a & . & a & a \\ a & a & a & a & . & a \\ a & a & a & a & a & . \end{pmatrix}. \tag{13}$$

This matrix is invariant to any permutation of indices, and the appropriate group of the matrix is $\mathscr{S}_6$, the symmetric group on six objects [17]. Here the 6 objects are *not the* CH *fermion fragments*, but the 6 indistinguishable $C_9H_9^+$ *fermions*, proposed to be connected *via* the common intermediate. Just as we may write determinantal wave functions for valence bond structures and combine configurations to produce a symmetry-correct state function, so we may write a wave function for the collection of isomers as a combination of functions typical of each isomer [cf. Eq. (5)]. If the nuclear spin state of each *isomer* is well defined, then the *system* wave function must be antisymmetric with respect to every feasible exchange of isomers, i.e., must belong to $[1^6]$. The individual isomers may have a total nuclear spin of 1/2, 3/2, ..., 9/2, and the total nuclear spin must be unchanged upon passage of a system from isomer to isomer, just as the total electronic spin must be the same in each valence bond electronic structure. Therefore the spin part of the total wave function is totally symmetric with respect to permutation of isomer labels; $\Gamma_{\text{spin}} = [6]$. Equation (13) has the form of the secular equation describing the mixing of the isomer functions, and the eigenvectors have the symmetry of the motional states. There are two eigenvalues, $+5a$, nondegenerate and spanning [6], and $-a$, fivefold degenerate and spanning [5 1]. The Pauli condition is: $\Gamma_{\text{total}} = \Gamma_{\text{motion}} \times \Gamma_{\text{ns}} = [1^6]$. This condition is not fulfilled by *any* combination of spin and motional states. *Therefore the* $\mathscr{D}_{3h}$ *structure is rigorously excluded as the transition state in the rearrangement process*, in that it leads to zero statistical weight for the fluxional state. Of course, structure **III** may still be the preferred structure of barbaralyl cation in solution, but the available computations are not able to settle this question definitively.

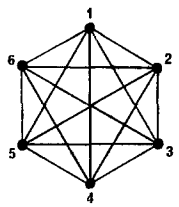

Fig. 5. Complete graph generated by proposed $\mathscr{D}_{3d}$ intermediate

Finally, it is interesting to note in connection with the $\mathscr{D}_{3d}$ structure that, while it is allowed as a transition state by conventional orbital symmetry arguments, it is excluded according to McIver's rules [18] for transition-state symmetry as well as by our analysis. Some caution is thereby indicated in relying only on conventional symmetry arguments, in that more subtle constraints may be overlooked.

9. Mechanism 2: Preliminary Remarks

The appropriate permutation group for Mechanism 2 is the symmetric group on nine particles, $\mathscr{S}_9$, with 362,880 elements [17], regardless of the assumed intermediate species [7]. All 9! degenerate isomers would eventually appear, with complete statistical equivalence of all protons. Spin states for the system span irreducible representations $^{10}[9]$, $^{8}[8\,1]$, $^{6}[7\,2]$, $^{4}[6\,3]$, and $^{2}[5\,4]$. On a time scale in which the Pauli principle applies to the nuclei, the total wave function must belong to $[1^9]$. In the ground vibronic state, the state corresponding to the rearrangement process would have to belong to the representation conjugate to that of the spin state.

The explicit solution of the kinetic equations involves the formation and diagonalization of a 9!x9! matrix, corresponding to the coupled rate Eqs. (14):

$$\frac{dC_i}{dt} = a(C_j + C_k + C_\ell + C_m + C_n + C_p) + bC_q - (6a+b)\,C_i\,, \tag{14}$$

where here the rate constants a and b refer to the rearrangement through the 1,2-vinyl shift and the Cope process, respectively.

The form of these equations implies that a given isomer is "adjacent" to six others by means of 1,2-vinyl shifts. We have generated the first 500 isomers produced from **I** on a computer. The partial graph, shown in Fig. 6, exhibits two levels of local structure. Isomers are joined, in groups of four, into tetrahedral subgraphs; each isomer belongs to two such tetrahedra, thereby satisfying the degree of six. The tetrahedra in turn are joined into six-membered rings, such that isomers on opposite sides of the ring are related by the Cope permutation. The latter has been excluded as a separate process from Fig. 6. A partial "graph of tetrahedra" is shown in Figs. 6b, c. This structure repeats throughout, but the graph of course eventually closes on itself.

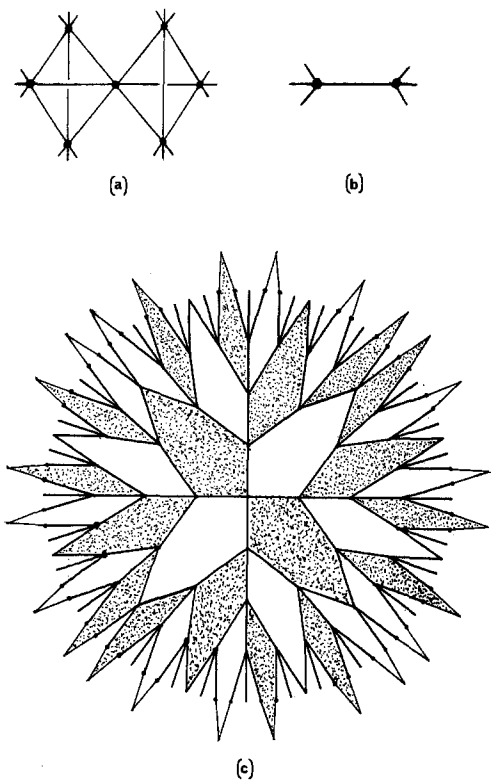

Fig. 6a–c. Partial graph for Mechanism 2. (a) Tetrahedral subgraphs formed by locally adjacent isomers. (b) Graph of tetrahedra in (a). Each point represents a tetrahedron; thus an isomer falls on the midpoint of an edge. (c) Partial graph of tetrahedra, showing all cyclic structures found within 5 steps from the reference tetrahedron. Opposite edges of shaded six-membered rings represent isomers related in the same way as structures **I** and **I'** of Fig. 1a

Although explicit solution of Eqs. (14) is impracticable, we are nonetheless able to extract considerable information from the properties of $\mathscr{S}_9$. The 9! isomers are in one-to-one correspondence with the group elements of $\mathscr{S}_9$. The elements of any group form a basis for the *regular representation* (Ref. [17], p. 107) of the group. The eigenvectors of the kinetic matrix – and indeed, of the microscopic secular matrix – therefore span all of the irreducible representations of the group, each as often as its degeneracy. For $\mathscr{S}_9$, the 30 irreducible representations and their degeneracies are listed in Table 4. All the relaxation times will be determined by specifying the two parameters a and b. Again there will be one mode, belonging to [9], with zero relaxation time implying conservation of mass. Furthermore, a theorem from the theory of graphs [19] implies that the distribution of eigenvalues is equally weighted about the constant multiplying the unit matrix (here $6a+b$), and that the maximum deviation from this value is the same constant. Hence all the kinetic relaxation times lie between 0 and $12a+2b$.

Table 4. Symmetry species and degeneracies for $\mathscr{S}_9$[a]

Representation	Degeneracy	Representation	Degeneracy
$[9]^b$, $[1^9]^c$	1	$[5\,3\,1]$, $[3\,2^2\,1^2]$	162
$[8\,1]^b$, $[2\,1^7]^c$	8	$[5\,2^2]$, $[3^3\,1^3]$	120
$[7\,2]^b$, $[2^2\,1^5]^c$	27	$[5\,2\,1^2]$, $[4\,2\,1^3]$	189
$[7\,1^2]$, $[3\,1^6]$	28	$[4^2\,1]$, $[3\,2^2]$	84
$[6\,3]^b$, $[2^3\,1^3]^c$	48	$[4\,3\,2]$, $[3^2\,2\,1]$	168
$[6\,2\,1]$, $[3\,2\,1^4]$	105	$[4\,3\,1^2]$, $[4\,2^2\,1]$	216
$[6\,1^3]$, $[4\,1^5]$	56	$[5\,1^4]$	70
$[5\,4]^b$, $[2^4\,1]^c$	42	$[3^3]$	42

[a] D. E. Littlewood, Theory of group characters, 2nd Ed., Clarendon 1950.
[b] Representations spanned by nuclear spin states.
[c] Motional states compatible with Pauli restriction.

The same argument applies to the microscopic stationary states. There will be a band of states centered on each vibrational level, with eigenvalues $|\lambda_i| \leqq 6a+b$. Because of the large number of states, and the probable total splitting of the order of a few cm^{-1}, the band approximates a continuum, with bandwidth of the order of $12a+2b$.

The Pauli compatibility condition is: $\Gamma_{\text{motion}} \times \Gamma_{\text{spin}} = [1^9]$. Reference to Table 4 shows that only five symmetry types of motional state are accessible: $[1^9]$, $[2\,1^7]$ (8 times), $[2^2\,1^5]$ (27 times), $[2^3\,1^3]$ (48 times), and $[2^4\,1]$ (42 times). Statistical weights of the motional states are given by $g \times (2I+1)$, where g is the number of times that symmetry type appears, and $(2I+1)$ is the multiplicity of the compatible spin state. The total weights for particular symmetries are: $[1^9]$:10, $[2\,1^7]$:64, $[2^2\,1^5]$:162, $[2^3\,1^3]$:192, and $[2^4\,1]$:84.

10. Discussion

One striking result of the symmetry analysis is that the structure imposed on the system by the group properties allows a great deal of information to be determined by only one or two numerical parameters. Thus, the macroscopic kinetic behavior, as well as the microscopic splitting of states, are in principle derivable from the results of one or two well-chosen experiments.

Leone *et al.* [5] conclude from experimental evidence that Mechanism 1 is the primary (and most rapid) process occurring, with some admixture of Mechanism 2. The symmetry analysis allows distinction between the two mechanisms provided that line shapes can be sufficiently resolved. It is clear that the Pauli condition severely restricts the number of motional states that can be occupied in Mechanism 2: out of the original 362,880 states, there remain only 4862 that can be populated, distributed among 126 distinct energy levels.

Recent experiments [20, 21] have indicated the possibility of observing effects of "frozen-in" nuclear spin population distribution on tunneling processes, through line shape analysis. Experiments such as these hold out the hope of observing statistical weight distributions which would make a mechanistic choice possible. Willem *et al.* [22] have described a multiple resonance method

for the determination of the relative probability of alternate rearrangement modes. This method can be applied without substantial change to determine the relative importance of $\mathscr{S}_9$ and $\mathscr{C}_{3v}$ mechanisms, but only if experimental conditions can be attained so that the characteristic time for the vinyl shift is greater than the transverse relaxation time. Finally, an experimental investigation of possible low-frequency transitions associated with motional states would provide impetus for a broader inquiry into the role of subtle symmetries in elucidating chemical reactions.

Acknowledgements. This work was supported by NSF grant GP-30817, and by the Office of Research and Projects of Southern Illinois University at Edwardsville. We thank Ms. Marian Whitfield for her assistance in generating groups and graphs, and Mr. Murray Brockman for a helpful discussion. TDB is grateful to the Department of Chemistry at the University of Virginia for its hospitality during the summers of 1972 and 1973.

References

1. Matsen, F.A.: J. Am. Chem. Soc. **92**, 3525 (1970)
2. Farkas, A.: Orthohydrogen, parahydrogen, and heavy hydrogen. Cambridge: University Press 1935
3. Trindle, C., Bouman, T.D.: Intern. J. Quantum Chem. Symp. **7**, 329 (1973)
4. Trindle, C., Bouman, T.D.: In: Sixth Jerusalem Symposium on Chemical and Biochemical Reactivity. Israel Academy of Sciences and Humanities 1974, p. 51
5. Leone, R.E., Barborak, J.C., Schleyer, P.v.R.: In: Carbonium ions, Olah, G.A., Schleyer, P.v.R., Eds., Vol. IV, Chapter 33. New York: Wiley 1973
6. Hoffmann, R., Stohrer, W.D., Goldstein, M.J.: Bull. Chem. Soc. Japan **45**, 2513 (1972)
7. Yoneda, S., Winstein, S., Yoshida, A.: Bull. Chem. Soc. Japan **45**, 2510 (1972)
8. Ahlberg, P., Harris, D.L., Winstein, S.: J. Am. Chem. Soc. **92**, 4454 (1970)
9. Ruch, E., Hässelbarth, W.: Theoret. Chim. Acta (Berl.) **29**, 259 (1973)
10. Klemperer, W.G.: J. Am. Chem. Soc. **94**, 6940 (1972)
11. Longuet-Higgins, H.C.: Mol. Phys. **6**, 445 (1963)
12. Dalton, B.J.: Mol. Phys. **11**, 265 (1966)
13. Brocas, J.: Theoret. Chim. Acta (Berl.) **21**, 79 (1971); Topics Current Chem. **32**, 43 (1972)
14. Wild, U., Keller, J., Günthard, H.H.: Theoret. Chim. Acta (Berl.) **14**, 383 (1969)
15. Stejskal, E.O., Gutowsky, H.S.: J. Chem. Phys. **28**, 388 (1958)
16. Woodman, C.M.: Mol. Phys. **11**, 109 (1966)
17. Hamermesh, M.: Group theory. Reading, Mass.: Addison-Wesley 1962
18. McIver, J.W., Jr.: Accounts Chem. Res. **7**, 72 (1974)
19. Behzad, M., Chartrand, E.: Introduction to the theory of graphs. Rockleigh, N.J.: Allyn and Bacon 1971
20. Clough, S., Hinshaw, W.S., Hobson, T.: Phys. Rev. Letters **31**, 1375 (1973)
21. Johnson, C.S., Jr., Mottley, C.: Chem. Phys. Letters **22**, 430 (1973)
22. Willem, R., Verdin, P., Brocas, J.: Bull. Soc. Chim. Belg. **83**, 37 (1974)

Prof. Thomas D. Bouman
Department of Chemistry
Southern Illinois University
Edwardsville, IL 62025
USA